Journal of Nutritional Dietetics & Probiotics
ISSN: 2640-6624

Chembio Publishers
Right Choice for Researchers

Research Article *Volume 2; Issue 2*

Physicochemical, Thermal, and Spectroscopic Characterization of the Consciousness Energy Healing Treated Cholecalciferol

Mahendra Kumar Trivedi[1] and Snehasis Jana[2]*

[1]Trivedi Global, Inc., Henderson, USA

[2]Trivedi Science Research Laboratory Pvt. Ltd., Thane (W), India

***Corresponding author:** Snehasis Jana, Trivedi Science Research Laboratory Pvt. Ltd., Thane (W), Maharashtra, India, Tel: +91-022-25811234; Email: publication@trivedieffect.com

Received Date: May 02, 2019; **Published Date:** May 10, 2019

Abstract

Cholecalciferol (Vitamin D_3) is used in the nutraceuticals for the prevention and treatment of vitamin D deficiency. This study was performed to determine the impact of The Trivedi Effect®-Consciousness Energy Healing Treatment on the physicochemical, thermal, and spectral properties of cholecalciferol using modern analytical techniques. Cholecalciferol was divided into two parts and termed as a control and treated sample. The treated part only received the Trivedi Effect®-Consciousness Energy Healing Treatment remotely by the famous Biofield Energy Healer, Mr. Mahendra Kumar Trivedi. The powder X-ray diffraction data revealed that the relative peak intensities and the crystallite size of the treated sample were significantly altered ranging from -58.97% to 25.95% and -55.52% to 53.84%, respectively, along with 23.32% decrease in the average crystallite size compared to the control sample. The latent heat of fusion and latent heat of decomposition of the Biofield Energy Treated cholecalciferol were decreased by 4.21% and 4.51%, respectively compared to the control sample. Besides, the particle size values of treated sample were significantly increased by 659.11% (d_{10}), 594.44% (d_{50}), 509.83% (d_{90}), and 570.55% {D(4,3)}, respectively compared to the control sample. Therefore, the specific surface area of the treated cholecalciferol was significantly reduced by 81.67% compared to the control sample. Thus, it was anticipated that the Trivedi Effect® might have produced the novel polymorphs of cholecalciferol *via* the possible mediation of neutrinos that could be helpful in improving the shape, size, appearance, and powder flow ability. Thus, the Biofield Energy Treated cholecalciferol could be useful in designing more efficacious nutraceutical and pharmaceutical formulations that may have improved therapeutic response against vitamin D deficiency and associated diseases such as, osteoporosis, rickets, cancer, etc.

Keywords: Cholecalciferol; The Trivedi Effect®; Energy of Consciousness Healing Treatment; PXRD; DSC; TGA; PSA

Abbreviations: PXRD: The Powder X-Ray Diffraction; PSD: The Particle Size Distribution; FT-IR: Fourier Transform Infrared; TGA: Thermal Gravimetric Analysis; DTG: Differential Thermo gravimetric Analysis; DSC: Differential Scanning Calorimetric; PSD: Particle Size Distribution

Introduction

Vitamin D plays a vital role in the human body as it helps in calcium metabolism and thereby essential for bone health throughout life. It also helps in maintaining the levels of calcium and phosphorous within the serum by enhancing their absorption. The process takes place along

Citation: Mahendra Kumar Trivedi and Snehasis Jana. Physicochemical, Thermal, and Spectroscopic Characterization of the Consciousness Energy Healing Treated Cholecalciferol. J Nutri Diet Probiotics 2019, 2(1): 180016.

with the help of parathyroid hormone that further enables bone mineralization. Several studies reported the association between the status of vitamin D in the body with bone mineral density, lower-extremity function, and fracture prevention, etc. [1]. There is some emerging evidence that also supports the impact of vitamin D on rheumatoid arthritis, type 1 diabetes, hypertension, cardiovascular disease, multiple sclerosis, common cancers, periodontal health, and colorectal cancer [2-4]. In cancer research, several epidemiological studies reported the role of vitamin D in the pathogenesis as well as the progression of cancer. Its active metabolite, calcitriol (1,25-dihydroxyvitamin D_3), is known to possess pro-apoptotic, ant proliferative, and pro-differentiating effects; therefore imparts the anti-inflammatory effects, along with inhibiting the NF-κB signaling, and suppressing the prostaglandin metabolism, tumour metastasis, and angiogenesis [5]. Cholecalciferol (vitamin D_3) is the natural form of vitamin D which is made by the body from sunlight. It is known to play an important role in improving the absorption of various minerals in the body such as calcium, magnesium, zinc, iron, and phosphate [6]. The studies reported that in nowadays, various people are not meeting the recommended dietary intakes for vitamin D [7]. Also, according to survey data, most of the people over 50 years do not get the adequate intake of vitamin D and calcium [8]. The causes behind low vitamin D status are limited exposure to sunlight, obesity, age-related decrease in the synthesis of vitamin D through the skin, use of sunscreens, and low intake of milk as well as the vitamin D-fortified foods [9]. Also, there are only a few foods that are naturally rich in vitamin D such as oily fish (e.g., mackerel, salmon, and herring) and cod liver oil. Therefore, vitamin D fortification of food and supplements is considered an important public health strategy [4]. Vitamin D_3 is air and light sensitive compound, which creates concern about the stability of this compound [10,11]. Since the physicochemical properties of a compound are important regarding its absorption, bioavailability, and stability profile [12]. The main focus of researchers is to improve these parameters of the compound. In this scenario, it was reported that the Biofield Energy Healing Treatment (the Trivedi Effect®) has a considerable effect on various properties of a drug such as crystallite size, particle size, surface area, and other chemical and thermal behaviour [13-15]. Every living organism is known to possess unique energy, which is infinite, para-dimensional and surrounds the body in the form of the electromagnetic field, known as Biofield Energy. There are several Biofield (Putative Energy Fields) based Energy Healing Therapies that are known to possess significant results against various disease conditions [16]. Thus the National Institutes of Health/National Center for Complementary and Alternative Medicine (NIH/NCCAM) recommend such Energy therapy under the category of Complementary and Alternative Medicine (CAM) [17]. The Trivedi Effect®-Consciousness Energy Healing treatment has been widely known for its impact on alteration of the physicochemical properties of pharmaceutical products [18,19], organic compounds, metals, and ceramics [20-22], nutraceutical [23,24], agricultural science [25, 26], livestock [27], and skin health [28, 29] may be *via* the possible mediation of neutrinos. Thus, this study was designed to analyse the impact of the Biofield Energy Healing Treatment on the physicochemical, thermal and spectral properties of cholecalciferol by using various sophisticated analytical techniques.

Materials and Methods

Chemicals and reagents

The test sample cholecalciferol (Sigma-Aldrich) and other chemicals used during the experiments were of analytical grade purchased in India.

Consciousness energy healing treatment strategies

The test compound, i.e., cholecalciferol was taken and divided into two parts. In this, one part did not receive the Biofield Energy Treatment and named as control cholecalciferol. Besides, the other part of the test compound received the Consciousness Energy Healing Treatment by the renowned Biofield Energy Healer, Mr. Mahendra Kumar Trivedi (USA), and it was considered as the Biofield Energy Treated cholecalciferol. In this process, the sample was placed under the standard laboratory conditions and the Healer provided the Trivedi Effect® - Consciousness Energy Healing Treatment remotely for three minutes through his unique energy transmission process. Consequently, the control sample was subjected to a "sham" healer under similar laboratory conditions, who did not have any knowledge about the Biofield Energy Treatment. Later both the samples were kept in similar sealed conditions and characterized with the help of analytical techniques.

Characterization

The powder X-ray diffraction (PXRD) analysis of cholecalciferol powder sample was performed with the help of PANalytical X'Pert3 Pro [30,31]. The average size of crystallites was calculated from PXRD data using the Scherrer's formula (1)

$$G = k\lambda/\beta\cos\theta \qquad (1)$$

Where G is the crystallite size in nm, k is the equipment constant (0.5), λ is the radiation wavelength (0.154 nm for Kα1 emission), β is the full-width at half maximum, and θ is the Bragg angle [32,33]. The particle size distribution (PSD) analysis was performed with the help of Malvern Mastersizer 3000, UK instrument and Mastersizer V3.50 software using the wet method [30,31]. Similarly, the differential scanning calorimetry (DSC) analysis of cholecalciferol was performed with the help of DSC Q200, TA instruments. The thermal gravimetric analysis (TGA) thermograms of cholecalciferol were obtained with the help of TGA Q50 TA instruments [30,31]. Fourier transform infrared (FT-IR) spectroscopy of cholecalciferol was performed on Spectrum ES (Perkin Elmer, USA) Fourier transform infrared spectrometer. Ultra violet-visible spectroscopy (UV-Vis) analysis was carried out using Shimadzu UV-2400PC series, Japan.

The % change in crystallite size, peak intensity, particle size, surface area, melting point, latent heat, weight loss and the maximum thermal degradation temperature of the Biofield Energy Treated cholecalciferol was calculated compared with the control sample using the following equation 2

$$\% \text{ Change} = \frac{[\text{Treated} - \text{Control}]}{\text{Control}} \times 100 \quad (2)$$

Statistical analysis

Data was represented as mean ± standard error of mean (SEM). Student's t-test was used to compare two groups to judge the statistical significance. Statistically significant values were set at the level of $p \leq 0.05$.

Results and Discussion

Powder X-ray diffraction (PXRD) analysis

There were sharp and intense peaks in the PXRD diffractograms of the control and Biofield Energy Treated cholecalciferol (Figure 1), which showed that both the samples were crystalline in nature. Moreover, the data regarding Bragg angle and other PXRD data such as d-spacing of the control sample were found to be in accordance with the reported literature for cholecalciferol [11]. Later on, the PXRD data that were collected from the diffractograms, such as Bragg angle (2θ), and relative peak intensity (%) of both the control and Biofield Energy Treated cholecalciferol. In this regard, the Scherer equation [32,33] was used for calculating the crystallite sizes across various planes.

Entry No.	Bragg angle (°2θ)	Relative Intensity (%)			Crystallite size (G, nm)		
		Control	Treated	% change	Control	Treated	% change
1	4.9	53.14	26.65	-49.85	57.36	43.06	-24.93
2	5.10	36.82	22.08	-40.03	49.23	43.07	-12.51
3	6.70	9.15	8.69	-5.03	31.34	28.72	-8.36
4	8.60	7.31	5.02	-31.33	28.75	26.54	-7.69
5	8.90	6.42	4.58	-28.66	26.55	28.76	8.32
6	13.00	15.76	9.3	-40.99	26.64	26.64	0.00
7	13.60	17.59	16.74	-4.83	28.88	21.65	-25.03
8	15.50	32.77	21.34	-34.88	86.76	38.59	-55.52
9	15.80	41.64	20.56	-50.62	31.58	31.58	0.00
10	16.20	22.4	9.19	-58.97	26.73	24.82	-7.15
11	16.70	8.67	10.92	25.95	43.49	31.62	-27.29
12	18.00	100	100	0.00	24.88	26.80	7.72
13	21.80	18.74	19.7	5.12	58.37	29.20	-49.97
14	23.60	12.99	9.79	-24.63	58.55	29.30	-49.96
15	27.00	5.35	4.67	-12.71	17.70	27.22	53.84
16	Average crystallite size				39.79±4.04	30.51±1.63	-23.32

Table 1: PXRD data for the control and Biofield Energy Treated cholecalciferol.

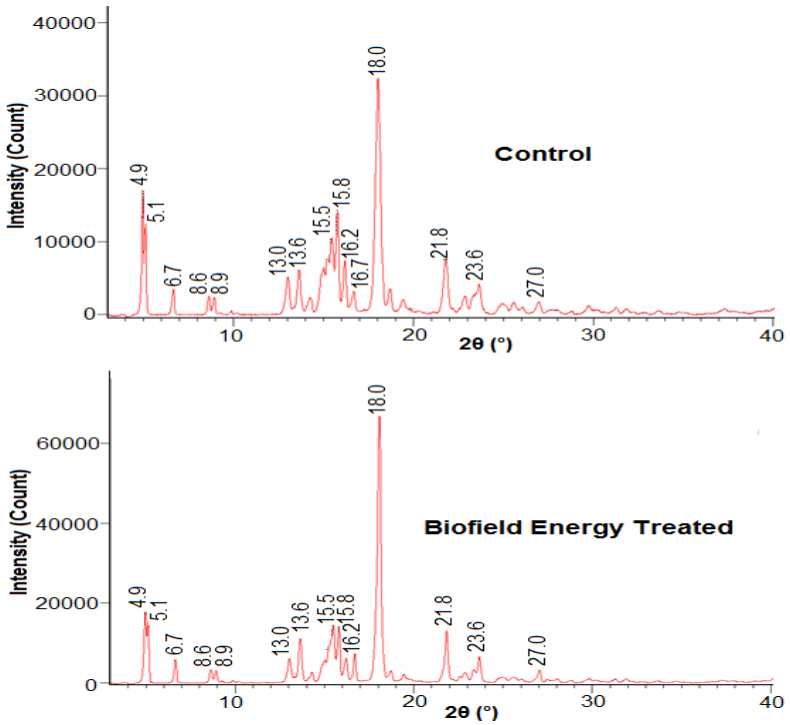

Figure 1: PXRD diffractograms of the control and Biofield Energy Treated cholecalciferol.

The PXRD diffractograms of the control and Biofield Energy Treated samples showed the highest peak intensity (100%) at Bragg's angle (2θ) equal to 18.0° (Table 1, entry 12). Besides, the relative peak intensities of the in the Biofield Energy Treated sample were significantly altered ranging from -58.97% to 25.95% compared to the control sample (Table 1, entry 1-13). On the other hand, the crystallite sizes of the Biofield Energy Treated sample were significantly altered ranging from -55.52% to 53.84% compared to the control sample. Also, the average crystallite size of the Biofield Energy Treated sample was found to be 30.51 nm, which was 23.32% less as compared to the crystallite size of the control sample (39.79nm). Such significant alterations in the relative intensities and crystallite size indicated that there was some modification in the crystal morphology of the Biofield Energy Treated cholecalciferol, compared to the control sample. It was previously reported that Biofield Energy Treatment might create a polymorph of the compound by modifying its crystal morphology with the help of changing the crystallite size and relative intensities of the diffraction peaks [34,35]. Thus, it could be presumed that the Trivedi Effect®-Energy of Consciousness Healing Treatment probably introduced a polymorphic form of the cholecalciferol through the energy transferring process. Moreover, the polymorphs of the compound have significant effects on drug performance, such as therapeutic efficacy and bioavailability due to the difference in their physicochemical and thermodynamic properties [36,37]. Hence, the Biofield Energy Treatment might be used as a technique for introducing the new crystal polymorph of cholecalciferol that would improve its drug performance.

Thermal gravimetric analysis (TGA) / Differential thermogravimetric analysis (DTG)

The TGA/DTG analysis is used for the determination of thermal stability of the samples by using the thermograms of the control and Biofield Energy Treated cholecalciferol (Figures 2 and 3). Also, the TGA and DTG data for the control and Biofield Energy Treated samples are mentioned in Table 2. According to literature, the TGA curve of cholecalciferol showed a significant weight loss at 128°C, which might be assigned to the boiling and thereby the possible splattering of the sample [11]. In this study, the TGA thermo grams of the control and Biofield Energy Treated cholecalciferol showed two steps of thermal degradation (Figure 2). The percentage weight loss in Biofield Energy Treated cholecalciferol sample was observed to be significantly increased by 9.67% and 0.70% in the 1st and 2nd step of degradation, respectively compared with the control sample (Table 2).

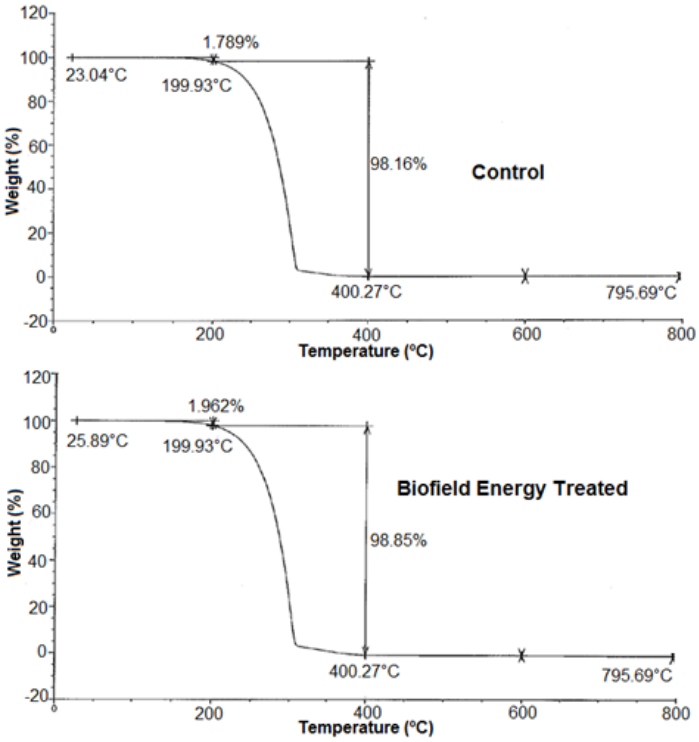

Figure 2: TGA thermograms of the control and Biofield Energy Treated cholecalciferol

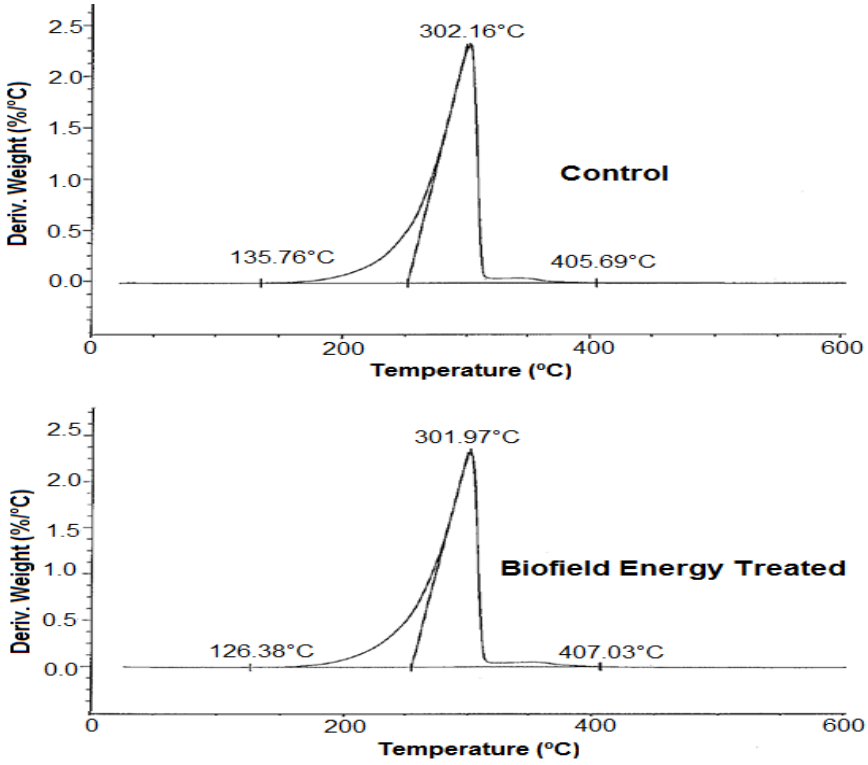

Figure 3: DTG thermograms of the control and Biofield Energy Treated cholecalciferol.

Sample	TGA Weight loss (%)			DTG
	1st step	2nd step	Total	T_{max} (°C)
Control	1.78	98.16	99.94	302.16
Biofield Energy Treated	1.96	98.85	100.0	301.97
% Change	9.67	0.703	0.06	-0.06

T_{max}: Maximum thermal degradation temperature.
Table 2: Thermal degradation steps and TGA/DTG data of the control and Biofield Energy Treated cholecalciferol.

Moreover, the DTG thermograms of the control and Biofield Energy Treated samples (Figure 3) exhibited a single peak. It was observed that the maximum thermal degradation temperature (T_{max}) for Biofield Energy Treated sample was 301.97°C, while the control sample showed slight more stability and T_{max} was found at 302.16°C. Thus, the T_{max} of the Biofield Energy Treated sample was slightly lowered by 0.06% as compared to the control sample. Overall, the TGA/DTG analysis revealed that the thermodynamic stability of the Biofield Energy Treated cholecalciferol was decreased as compared to the control sample.

Differential scanning calorimetry (DSC) analysis

The DSC analysis was used for the analysis of melting point and latent heat of fusion (ΔH) of the control and Biofield Energy Treated samples. The DSC thermo grams of control and Biofield Energy Treated cholecalciferol are shown in Figure 4 and related data are presented in Table 3. The DSC thermograms of both, the control and Biofield Energy Treated cholecalciferol samples (Figure 4) exhibited two endothermic and one exothermic peak. It was previously reported that the sharp endothermic peak present near 86.0° in the DSC curve is due to the melting of cholecalciferol; while the exothermic peak present near 220°C may be due to the decomposition of cholecalciferol [11]. This study showed that the melting point of the Biofield Energy Treated sample (86.25°C) was slightly increased by 0.61% compared to the control sample (85.73°C). However, the latent heat of fusion (ΔH) of the Biofield Energy Treated sample was found to be decreased by 4.21% compared with the control sample. Thus, it could be presumed that the Biofield Energy Treated cholecalciferol sample needs less energy in the form of ΔH to undergo the melting process. Consequently, the decomposition temperature and the latent heat of decomposition (2nd peak) of the Biofield Energy Treated sample were observed to be decreased by 0.23% and 4.51%, respectively, compared with the control sample.

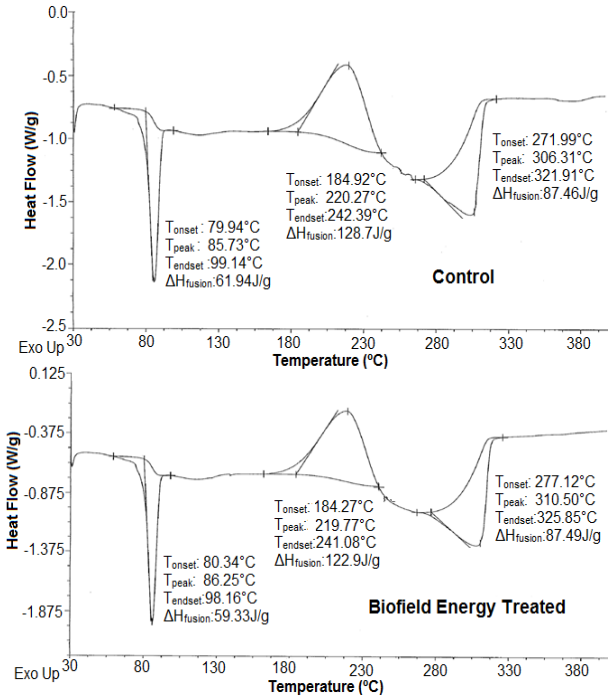

Figure 4: DSC thermograms of the control and Biofield Energy Treated cholecalciferol.

Sample	Melting/Decomposition Temperature (°C)			ΔH (J/g)		
	1st Peak	2nd Peak	3rd Peak	1st Peak	2nd Peak	3rd Peak
Control	85.73	220.27	306.31	61.94	128.7	87.46
Biofield Energy Treated	86.25	219.77	310.50	59.33	122.9	87.49
% Change	0.61	-0.23	1.37	-4.21	-4.51	0.03

Table 3: Comparison of DSC data between the control and Biofield Energy Treated cholecalciferol.
ΔH: Latent heat of fusion/latent heat of decomposition.

Later on, the 2nd broad endothermic peak (3rd peak) at 306.31° in the control sample and 310.50° in the Biofield Energy Treated sample might represent the slow degradation of non-volatile intermediates that may develop during the thermal reaction. The temperature and ΔH of the Biofield Energy Treated sample corresponding to this peak were found to be increased by 1.37% and 0.03%, respectively (Table 3) compared to the control sample. The overall results suggested that the thermodynamic stability of the Biofield Energy Treated sample was significantly altered as compared to the control sample.

Fourier transform infrared (FT-IR) spectroscopy

The FT-IR spectra of both the control as well as Biofield Energy Treated cholecalciferol samples are presented in Figure 5. The FT-IR spectra of both the samples showed the clear stretching and bending peak in the functional group and fingerprint region.

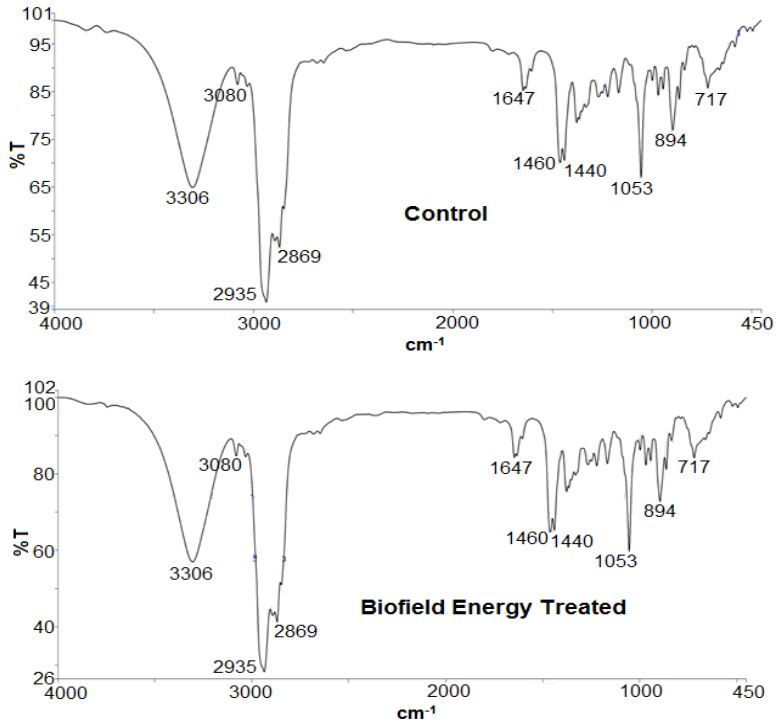

Figure 5: FT-IR spectra of the control and Biofield Energy Treated cholecalciferol.

The broad peaks near 3306cm^{-1} in the functional group area were observed in both control and Biofield Energy Treated spectra and were assigned to O-H stretching. The spectra showed aromatic C-H stretching at 3080 cm^{-1} in case of both, the control and Biofield Energy Treated samples. Also, there were aliphatic C-H stretching at 2935 cm^{-1} and 2869 cm^{-1} in the spectra of control as well as the Biofield Energy Treated sample. Besides, the variable peak observed at 1647cm^{-1} in the spectra of control and Biofield Energy Treated cholecalciferol samples were the results of C=C stretching. Moreover, both the spectra showed aromatic C=C stretching frequency at 1440 and 1460 cm^{-1}. The overall FT-IR analysis revealed that the fingerprint region of the spectra of control and Biofield

Energy Treated sample remained same and there were no changes in the vibrational frequencies. Thus, it could be assumed that there was no alteration in the structural properties of the Biofield Energy Treated sample as compared to the control sample.

Ultraviolet-visible spectroscopy (UV-Vis) analysis

The UV-visible spectra of both the control and biofield Energy Treated cholecalciferol samples are shown in Figure 6.

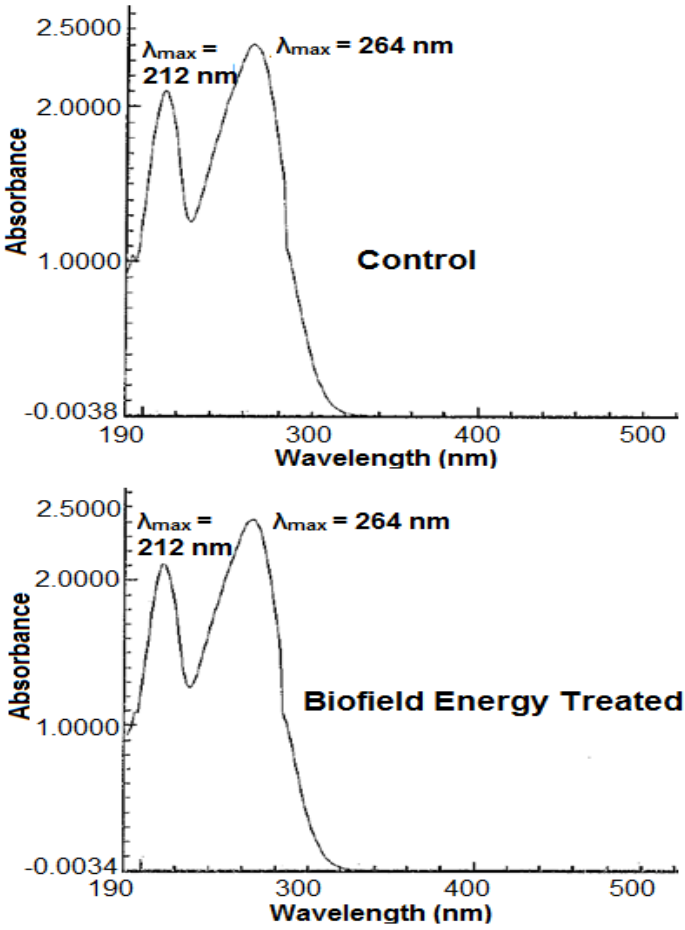

Figure 6: UV-vis spectra of the control and Biofield Energy Treated cholecalciferol.

The UV spectrum of both the control and Biofield Energy Treated sample showed the maximum absorbance at 212 nm (λ_{max}) and 264 nm (λ_{max}). Thus, the analysis revealed that the electronic transitions between the highest occupied molecular orbital and lowest unoccupied molecular orbital remained the same in the control and Biofield Energy Treated cholecalciferol sample.

Particle size distribution (PSD) analysis

Particle sizes (d_{10}, d_{50}, and d_{90}) and the surface area of the control and Biofield Energy Treated cholecalciferol samples were analysed and the results are mentioned in Table 4. The particle size distribution of the control sample was observed at d_{10}=7.68µm, d_{50}=32.40µm, d_{90}=65.10 µm, and D(4, 3) = 34.30 µm. Consequently, the particle size distribution of the Biofield Energy Treated sample was observed at d_{10}=58.30µm, d_{50}=225.0 µm, d_{90} = 397.0 µm, and D(4, 3)=230.0 µm. It revealed that the particle size values at d_{10}, d_{50}, and d_{90}, and D(4, 3) in the Biofield Energy Treated sample were significantly increased by 659.11%, 594.44%, 509.83%, and 570.55%, respectively compared to the control sample. Besides, the specific surface area (SSA) of the Biofield Energy Treated sample (57.84 m^2/Kg) was found to be significantly decreased by 81.67% as compared to the control sample (315.60 m^2/Kg).

Test Item	d_{10} (µm)	d_{50} (µm)	d_{90} (µm)	D(4,3) (µm)	SSA(m^2/Kg)
Control sample	7.68	32.40	65.10	34.30	315.60
Biofield Energy Treated sample	58.30	225.0	397.0	230.0	57.84
Percent change (%)	659.11	594.44	509.83	570.55	-81.67

Table 4: The particle size distribution of the control and Biofield Energy Treated cholecalciferol.
d_{10}, d_{50}, and d_{90}: particle diameter corresponding to 10%, 50%, and 90% of the cumulative distribution, D(4,3): the average mass-volume diameter, and SSA: the specific surface area.

Some studies reported that the elevation in the thermal energy may affect the particle size of the compound. Thus, it is presumed that the Biofield Energy Treatment might reduce the thermodynamically driving force that further decreases the nucleus densities and thereby enhances the particle size [38,39]. Moreover, the Biofield Energy Treated sample showed a reduction in the specific surface area as compared to the control sample that might be due to the enhanced particle size after the Biofield Energy Treatment. Moreover, the increased particle size of the compound may help in enhancing the appearance, shape, and flow ability of the compound [40, 41]. Thus, the Biofield Energy Treatment might be used as a measure to improve the powder flow ability of cholecalciferol.

Conclusions

The Trivedi Effect®-Energy of Consciousness Healing Treatment significantly affect the physicochemical and thermal properties, i.e., crystallite size, particle size, surface area, and thermodynamic properties of cholecalciferol. The powder X-ray diffraction data revealed that the relative peak intensities and the crystallite size of the Biofield Energy Treated sample were significantly altered ranging from -58.97% to 25.95% and -55.52% to 53.84%, respectively, along with 23.32% decrease in the average crystallite size compared to the control sample. Such changes in the relative intensities and crystallite size of the treated sample indicated that the Trivedi Effect®-Consciousness Energy Healing Treatment might produce a polymorphic form of the cholecalciferol with the help of energy transferring process. The latent heat of fusion and latent heat of decomposition of the Biofield Energy Treated cholecalciferol were decreased by 4.21% and 4.51%, respectively compared to the control sample. However, the particle size values of the Biofield Energy Treated sample were significantly increased by 659.11% (d_{10}), 594.44% (d_{50}), 509.83% (d_{90}), and 570.55% {D(4,3)}, respectively compared to the control sample. Therefore, the specific surface area of the Biofield Energy Treated cholecalciferol was significantly reduced by 81.67% compared to the control sample. Thus, it was anticipated that the Trivedi Effect® might have produced the novel polymorphs of cholecalciferol *via* the possible mediation of neutrinos that could be helpful in improving the shape, size, appearance, and powder flow ability. Thus, the Biofield Energy Treated cholecalciferol could be useful in designing more efficacious nutraceutical and pharmaceutical formulations against vitamin D deficiency associated diseases such as rickets, osteoporosis, rheumatoid arthritis, type 1 diabetes, hypertension, multiple sclerosis, cardiovascular disease, periodontal disease, and colorectal cancer.

Acknowledgements

The authors are grateful to GVK Biosciences Pvt. Ltd., Trivedi Science, Trivedi Global, Inc., Trivedi Testimonials, and Trivedi Master Wellness for their assistance and support during this work.

References

1. Institute of Medicine (1997) Dietary reference intakes for calcium, phosphorus, magnesium, vitamin D, and fluoride. Washington (DC): National Academy of Sciences.

2. Simana E, Simian R, Portnoy S, Jaffe A, Dekel BZ (2015) Feasibility Study-Vitamin D loading determination by FTIRATR. Information & Control Systems 76: 107-111.

3. Lawson DE, Wilson PW, Kodicek E (1969) Metabolism of vitamin D. A new cholecalciferol metabolite, involving loss of hydrogen at C-1, in chick intestinal nuclei. Biochem J 115(2): 269-77.

4. Ritu G, Gupta A (2014) Vitamin D Deficiency in India: prevalence, causalities and interventions. Nutrients. 6(2): 729-775.

5. Xu J, Li W, Ma J, Liu J, Sha H, et al. (2013) Vitamin D - pivotal nutraceutical in the regulation of cancer metastasis and angiogenesis. Curr Med Chem 20(33): 4109-4120.

6. Bikle DD (2014) Vitamin D metabolism, mechanism of action, and clinical applications. Chem Biol. 21(3): 319-329.

7. IOM (2008) The Development of DRIs 1994-2004: Lessons Learned and New Challenges: Workshop Summary. Washington, DC: The National Academies Press.

8. Bailey RL, Dodd KW, Goldman JA, Gahche JJ, Dwyer JT, et al. (2010) Estimation of Total Usual Calcium and Vitamin D Intakes in the United States. J Nutr. 140(4): 817-822.

9. Boucher BJ (2012) The Problems of Vitamin D Insufficiency in Older People. Aging Dis 3(4): 313-329.

10. Collins ED, Norman AW (2001) Vitamin D in Handbook of Vitamins. (3rd edn), Rucker RB, Suttie JW, McCormick DB, Machlin LJ, Marcel Dekker, Inc., New York, pp. 51-114.

11. Koshy KT, Beyer WF (1984) Vitamin D_3 (Cholecalciferol) in Analytical Profiles of Drug Substances, Florey K (Ed.), Vol 13, Academic Press, Inc., Orlando, USA, pp: 656-707.

12. Chereson R (2009) Bioavailability, bioequivalence, and drug selection. In: Makoid CM, Vuchetich PJ, Banakar UV (Eds) Basic pharmacokinetics (1st Edn), Pharmaceutical Press, London.

13. Hammerschlag R, Levin M, McCraty R, Bat N, Ives JA, et al. (2015) Biofield Physiology: A Framework for an Emerging Discipline. Glob Adv Health Med 4(Suppl): 35-41.

14. Warber SL, Cornelio D, Straughn, J, Kile G (2004) Biofield energy healing from the inside. J Altern Complement Med 10: 1107-1113.

15. Trivedi MK, Mohan TRR (2016) Biofield energy signals, energy transmission and neutrinos. American Journal of Modern Physics 5(6): 172-176.

16. Rubik B, Muehsam D, Hammerschlag R, Jain S (2015) Biofield science and healing: history, terminology, and concepts. Glob Adv Health Med 4(Suppl): 8-14.

17. Barnes PM, Bloom B, Nahin RL (2008) Complementary and alternative medicine use among adults and children: United States, 2007. Natl Health Stat Report 10(12): 1-23.

18. Trivedi MK, Branton A, Trivedi D, Shettigar H, Bairwa K, et al. (2015) Fourier transform infrared and ultraviolet-visible spectroscopic characterization of biofield treated salicylic acid and sparfloxacin. Nat Prod Chem Res 3: 186.

19. Trivedi MK, Patil S, Shettigar H, Bairwa K, Jana S (2015) Effect of biofield treatment on spectral properties of paracetamol and piroxicam. ChemSci J 6: 98.

20. Trivedi MK, Branton A, Trivedi D, Nayak G, Saikia G, et al. (2015) Thermal, spectroscopic and chromatographic characterization of biofield energy treated benzophenone. Science Journal of Analytical Chemistry 3(6): 109-114.

21. Trivedi MK, Nayak G, Patil S, Tallapragada RM, Latiyal O, et al. (2015) Evaluation of biofield treatment on physical and structural properties of bronze powder. Adv Automob Eng 4: 119.

22. Trivedi MK, Tallapragada RM, Branton A, Trivedi D, Nayak G, et al. (2015) Characterization of physical and structural properties of aluminum carbide powder: Impact of biofield treatment. J Aeronaut Aerospace Eng 4: 142.

23. Trivedi MK, Branton A, Trivedi D, Nayak G, Wellborn BD, et al. (2017) Characterization of physicochemical, thermal, structural, and behavioral properties of magnesium gluconate after treatment with the Energy of Consciousness. International Journal of Pharmacy and Chemistry 3(1): 1-12.

24. Trivedi MK, Branton A, Trivedi D, Nayak G, Balmer AJ, et al. (2017) Study of the energy of consciousness healing treatment on physical, structural, thermal, and behavioral properties of zinc chloride. Modern Chemistry 5(2): 19-28.

25. Trivedi MK, Branton A, Trivedi D, Nayak G, Gangwar M, et al. (2016) Molecular analysis of biofield treated eggplant and watermelon crops. Adv Crop Sci Tech 4(1): 208.

26. Trivedi MK, Branton A, Trivedi D, Nayak G, Mondal SC, et al. (2015) Evaluation of biochemical marker - Glutathione and DNA fingerprinting of biofield energy treated Oryza sativa. American Journal of BioScience 3(6): 243-248.

27. Trivedi MK, Branton A, Trivedi D, Nayak G, Mondal SC, et al. (2015) Effect of Biofield treated energized water on the growth and health status in chicken (Gallus gallusdomesticus). Poult Fish WildlSci 3:2-140.

28. Kinney JP, Trivedi MK, Branton A, Trivedi D, Nayak G, et al. (2017) Overall skin health potential of the biofield energy healing based herbomineral formulation using various skin parameters. American Journal of Life Sciences 5(2): 65-74.

29. Dodon J, Trivedi MK, Branton A, Trivedi D, Nayak G, et al. (2017) The study of biofield energy treatment based herbomineral formulation in skin health and function. American Journal of BioScience 5(3): 42-53.

30. Trivedi MK, Branton A, Trivedi D, Nayak G, Plikerd WD, et al. (2017) A systematic study of the biofield energy healing treatment on physicochemical, thermal, structural, and behavioral properties of iron sulphate. International Journal of Bioorganic Chemistry 2(3): 135-145.

31. Trivedi MK, Branton A, Trivedi D, Nayak G, Lee AC, et al. (2017) A comprehensive analytical evaluation of the Trivedi Effect® - Energy of Consciousness Healing Treatment on the physical, structural, and thermal properties of zinc chloride. American Journal of Applied Chemistry 5(1): 7-18.

32. Langford JI, Wilson AJC (1978) Scherrer after sixty years: A survey and some new results in the determination of crystallite size. J Appl Cryst 11(2): 102-113.

33. Brittain HG (2009) Polymorphism in pharmaceutical solids in Drugs and Pharmaceutical Sciences. (2nd Edn) Informa Healthcare USA, Inc., New York.

34. Trivedi MK, Branton A, Trivedi D, Nayak G, Lee AC, et al. (2017) investigation of physicochemical, spectral, and thermal properties of sodium selenate treated with the Energy of Consciousness (the Trivedi Effect®). American Journal of Life Sciences 5(1): 27-37.

35. Raza K, Kumar P, Ratan S, Malik R, Arora S (2014) Polymorphism: The phenomenon affecting the performance of drugs. SOJ Pharm Pharm Sci 1(2): 10.

36. Zhao Z, Xie M, Li Y, Chen A, Li G, et al. (2015) Formation of curcumin nanoparticles *via* solutionenhanced dispersion by supercritical CO_2. Int J Nanomedicine 10: 3171-3181.

37. Censi R, Martino PD (2015) Polymorph Impact on the Bioavailability and Stability of Poorly Soluble Drugs. Molecules 20(10): 18759-18776.

38. Rashidi AM, Amadeh A (2009) The effect of saccharin addition and bath temperature on the grain size of nanocrystalline nickel coatings. Surf Coat Technol 204(3): 353-358.

39. Katayama M (1956) The crystal structure of an unstable form of chloroacetamide. Acta Crystallogr 9(12): 986-991.

40. Mosharrof M, Nystrom C (1995) The effect of particle size and shape on the surface specific dissolution rate of microsized practically insoluble drugs. Int J Pharm 122(1-2): 35-47.

41. Buckton G, Beezer AE (1992) The relationship between particle size and solubility. Int J Pharmaceutics 82(3): R7-R10.